Neonatal Fc Receptor Mediates Internalization of Fc in Transfected Human Endothelial Cells

Nancy A. Goebl,* Clifford M. Babbey,† Amita Datta-Mannan,* Derrick R. Witcher,‡ Victor J. Wroblewski,* and Kenneth W. Dunn†

*Department of Drug Disposition Development/Commercialization, and ‡Biotechnology Discovery Research, Lilly Research Laboratories, Eli Lilly and Company, Indianapolis, IN 46285; and †Department of Medicine, Division of Nephrology, Indiana University Medical Center, Indianapolis, IN 46202

The neonatal Fc receptor, FcRn mediates an endocytic salvage pathway that prevents degradation of IgG, thus contributing to the homeostasis of circulating IgG. Based on the low affinity of IgG for FcRn at neutral pH, internalization of IgG by endothelial cells is generally believed to occur via fluid-phase endocytosis. To investigate the role of FcRn in IgG internalization, we used quantitative confocal microscopy to characterize internalization of fluorescent Fc molecules by HULEC-5A lung microvascular endothelia transfected with GFP fusion proteins of human or mouse FcRn. In these studies, cells transfected with FcRn accumulated significantly more intracellular Fc than untransfected cells. Internalization of FcRn-binding forms of Fc was proportional to FcRn expression level, was enriched relative to dextran internalization in proportion to FcRn expression level, and was blocked by incubation with excess unlabeled Fc. Because we were unable to detect either surface expression of FcRn or surface binding of Fc, these results suggest that FcRn-dependent internalization of Fc may occur through sequestration of Fc by FcRn in early endosomes. These studies indicate that FcRn-dependent internalization of IgG may be important not only in cells taking up IgG from an extracellular acidic space, but also in endothelial cells participating in homeostatic regulation of circulating IgG levels.

INTRODUCTION

The MHC class I–related Fc receptor FcRn mediates a number of functions in the trafficking of IgG. In rodents, FcRn in the neonatal gut epithelium and fetal yolk sac transports maternal IgG to the neonate (Rodewald and Kraehenbuhl, 1984; Roberts *et al.,* 1990) and in humans FcRn mediates maternal-fetal IgG transport across the placenta (Story *et al.,* 1994; Firan *et al.,* 2001). FcRn mediates transcytosis of IgG across absorptive epithelia in a variety of adult human tissues and cell lines including intestine (Israel *et al.,* 1997), kidney (Haymann *et al.,* 2000; Kobayashi *et al.,* 2002), and lung (Spiekermann *et al.,* 2002). FcRn has also been localized to white blood cells, including monocytes and macrophages (Zhu *et al.,* 2001) and has been proposed to play an important role in IgG-mediated phagocytosis in neutrophils (Vidarsson *et al.,* 2006).

FcRn has also been identified in endothelial tissue and cell lines (Ghetie *et al.,* 1996; Borvak *et al.,* 1998) in which it is believed to participate in an endocytic salvage pathway that prevents degradation of IgG, thus contributing to the homeostasis of circulating IgG (Ghetie *et al.,* 1996; Junghans and Anderson, 1996; Israel *et al.,* 1996; Ghetie and Ward, 2000, 2002). This salvage mechanism is believed to be responsible for the long half-life of IgGs in the circulation relative to other soluble proteins and peptides. The salvage

model is strongly supported by the observation that the serum half-life of IgG is significantly shortened in genetically engineered mice lacking functional FcRn (Ghetie *et al.,* 1996; Israel *et al.,* 1996; Junghans and Anderson, 1996) and also by studies indicating low serum IgG levels in individuals with deficient expression of FcRn (Wani *et al.,* 2006).

The mechanism by which FcRn is thought to mediate the salvage of IgG depends on the highly pH-dependent binding of IgG to FcRn (Rodewald and Kraehenbuhl, 1984; Junghans and Anderson, 1996; Ghetie and Ward, 2000, 2002). The binding affinity of FcRn for IgG is more than 100-fold higher at pH 6.0 than at pH 7.1 when measured by BIAcore surface plasmon resonance (SPR; Raghavan *et al.,* 1995). The high affinity of IgG for FcRn at acidic pH is believed to result in binding of internalized IgG to FcRn after uptake into acidic endosomes. Thus, although most soluble proteins are directed to lysosomes after internalization, internalized IgG would piggyback with the FcRn back to the plasma membrane and be effectively rescued from the default degradative pathway. On exposure to the neutral pH of the extracellular space, IgG would then dissociate from FcRn and return to the circulation. The system provides for IgG homeostasis in that IgG present at levels beyond that saturating the FcRn would not be captured into the recycling pathway and thus would be directed to the lysosomal pathway for degradation.

Based on the low affinity of IgG for FcRn at neutral pH, it is generally thought that internalization by endothelial cells occurs via fluid-phase endocytosis (Junghans and Anderson, 1996; Ghetie and Ward 2000). In addition, the fact that a relatively small fraction of the receptor is present on the cell surface (Borvak *et al.,* 1998; Antohe *et al.,* 2001; Spiekermann *et al.,* 2002; Claypool *et al.,* 2004; Stirling *et al.,* 2005;

Sakagami *et al.,* 2006) has been taken to suggest a limited potential for FcRn-mediated endocytosis of IgG. Because IgG is present in the serum at high concentrations (11–12 mg/ml in humans; Waldmann and Strober, 1969 and 1.5–8.0 mg/ml in mice; Ghetie *et al.,* 1996; Telleman and Junghans 2000), fluid-phase internalization, particularly by endocytically active endothelial cells, could support a significant avenue of cellular internalization in vivo.

Although the notion that the in vivo IgG salvage pathway depends on fluid-phase internalization is widely accepted in the literature, it has not been directly demonstrated. In fact, binding studies conducted by Gurbaxani *et al.* (2006) indicate that although the affinity of IgG for FcRn at neutral pH is weak, it may nonetheless be sufficient to support FcRn-mediated internalization of IgG at the high serum levels found in vivo. Calculations conducted by these authors indicated that under these conditions, binding at neutral pH may amount to 80–90% of that at pH 6.0.

Here we describe studies to address the role of FcRn in the internalization of IgG. HULEC-5A microvascular endothelial cells were transfected with green fluorescent protein (GFP) fusion constructs of mouse or human FcRn, allowing us to analyze early trafficking events of fluorescently labeled Fc fragment mutants by quantitative confocal microscopy. The sensitivity of this system enables visualization of cells after incubations brief enough to minimize the effects of recycling so that the amount of cell-associated Fc primarily reflects internalization. As expected, GFP-FcRn is found in endosomes of the recycling pathway, closely colocalizing with internalized transferrin (Tf). After brief internalization periods, Fc constructs are likewise largely associated with these same compartments, from which they recycle. Several lines of evidence indicate that FcRn mediates internalization of Fc in these cells. These studies indicate that FcRn-dependent internalization of IgG may be important not only in cells taking up IgG from an extracellular acidic space, but also in endothelial cells participating in homeostatic regulation of circulating IgG levels.

METHODS AND METHODS

Cells

HULEC-5A cells (SV-40 large T antigen–transformed human lung microvascular endothelial cells) were licensed from the Center for Disease Control and maintained in phenol red-free endothelial basal medium (Clonetics, San Diego, CA) and 10% ultra low IgG fetal bovine serum (Invitrogen, Carlsbad, CA) supplemented with 10 ng/ml mouse epidermal growth factor (Becton-Dickinson, San Diego, CA), 1 μg/ml hydrocortisone (Sigma, St. Louis, CA), 2 mM GlutaMax (Invitrogen), and penicillin/streptomycin. For fluorescence experiments, cells were grown on uncoated glass-bottom coverslip dishes (MatTek, Ashland, MA) and used between cell passages 16-23. Madin-Darby canine kidney (MDCK) cells (PTR clone, MDCK strain II cells stably transfected with the human TfR and the rabbit polymeric immunoglobulin receptor (pIgR; Brown *et al.,* 2000) were grown in phenol red-free MEM (Invitrogen), 10% ultra-low IgG fetal bovine serum (Invitrogen), 1% L-glutamine with penicillin/streptomycin (Sigma), and 0.05% hygromycin. Cells were grown as unpolarized monolayers on uncoated MatTek coverslip dishes.

Plasmids and Transfection

GFP-tagged human and mouse FcRn plasmids were generated in the bicistronic pIRES vector (BD Biosciences, San Jose, CA). Plasmids contained both the species specific α-FcRn subunit fused to a C-terminal enhanced GFP and the β2-microglobulin (β2m) subunit. These constructions permitted the translation of both α-FcRn-GFP and β2m from a single RNA transcript. To produce the final constructions, α-FcRn and enhanced GFP (EGFP) genes were first cloned into the pEGFP-N3 vector. The α-FcRn with C-terminal GFP was then cloned into the first pIRES multiple cloning site upstream of the internal ribosome entry site (IRES), whereas the β2m gene was cloned into the multiple cloning site downstream of the IRES site. The correct composition and alignment of all constructs was verified by sequencing. HULEC-5A cells were transfected using Lipofectamine 2000 (Invitrogen), and MDCK cells were transfected with Gene Jammer (Stratagene, La Jolla, CA) transfection reagent

according to the manufacturer's suggested protocols. Cells were transfected 40–48 h before fluorescent-labeling experiments.

Expression and Purification of Soluble hFcRn and mFcRn

Recombinant, soluble hFcRn and mFcRn were expressed in 293EBNA cells transfected with the plasmids encoding for the soluble portion of each receptor species αFcRn and β2m, and the proteins were purified as previously described (Datta-Mannan *et al.,* 2007).

Fc Reagents

The wild-type (WT) human Fc (IgG1) and T250Q/M428L and H435A Fc variants were expressed from 293EBNA cells and purified as follows. Expression media from 293EBNA cells containing the expressed Fc were concentrated and loaded onto a recombinant protein A-Sepharose prepacked column (GE Healthcare, Waukesha, WI) at a rate of 5 ml/min. The column was washed with 1 mM potassium phosphate, 3 mM sodium phosphate, 0.150 M NaCl, pH 7.4 (buffer A), until the absorbance returned to baseline. The Fcs were eluted with 100 mM glycine, pH 3.2, and fractions were neutralized using 40 μl Tris (pH 8.0) per milliliter of elution buffer. Fractions containing the Fcs were pooled and concentrated and loaded onto a Superdex 200 (26/60; GE Healthcare) sizing column equilibrated with buffer A at a flow rate of 3 ml/min. Fractions containing Fc were pooled and characterized by SDS-PAGE and mass spectrometry. Samples were sterile filtered (0.22 μm) and stored at 4°C.

Fluorescent Ligand Preparation

Alexa 647–labeled dextran (10 kDa, anionic, fixable) was obtained from Molecular Probes (Eugene, OR). Human transferrin was obtained from Sigma, iron-loaded and purified as described in Yamashiro *et al.* (1984), and then labeled with Cy5 (Amersham Pharmacia, Piscataway, NJ). Antibody Fc fragments were conjugated to Texas Red using the Texas Red-X Protein Labeling Kit (Molecular Probes) using 0.5–0.6 mg of protein per reaction. Labeled proteins were separated from unlabeled fluor using 20-cm P30 Biogel (Bio-Rad) size exclusion columns and ultracentrifuged at $100,000 \times g$ for 30 min. Protein concentration and degree of labeling were determined by spectrophotometry. Probes not used within 1 wk of preparation were stored at -20°C in single use aliquots.

Fc–FcRn Binding Affinity and Interaction Kinetics Measurements with Surface Plasmon Resonance (BIAcore)

The interaction kinetics of WT Fc and the T250Q/M428L and H435A variants with recombinant, immobilized hFcRn and mFcRn was monitored by SPR detection using a BIAcore 2000 instrument (Biacore, Piscataway, NJ) as previously described (Datta-Mannan *et al.,* 2007). Briefly, recombinant soluble hFcRn and mFcRn were immobilized to flow cells 2 and 3, respectively, of a CM5 sensor chip using amine-coupling chemistry. The surface density of each receptor species was 275-350 response units (RU). The first flow cell was used as a blank control surface lacking FcRn and was prepared as described previously. All binding experiments were performed with the WT Fc, and variants were dissolved in PBS, pH 6.0, and 0.005% (vol/vol) Tween 20 over a concentration range of 0.0033–4 μM as described for previous studies (Datta-Mannan *et al.,* 2007). Dissociation of the Fc was performed with either PBS, pH 6.0 or 7.4, and 0.005% (vol/vol) Tween 20. The binding data were obtained by subtracting the signal of flow cell 1 from the other two flow cells. Kinetic binding constants for experiments conducted at pH 6.0 were determined through global fits of the average of two data sets collected on separate days using BIAevaluation, version 3.1. The kinetics (association and dissociation rates) were then simultaneously fit to a heterogeneous binding model to determine the equilibrium dissociation constant (K_d) value for each FcRn–IgG interaction. The data curves for binding and dissociation phases of the sensorgrams for the WT and variant Fcs at pH 6.0 had low residuals and χ^2 values. For experiments in which Fc binding to FcRn was conducted at pH 6.0 and dissociation at pH 7.4, the rates of dissociation of the WT and variants was estimated by fitting the dissociation phase of each curve independent of the binding phase. Binding of the WT and variants to human and mouse FcRn was also tested with each Fc dissolved in PBS, pH 7.4, and 0.005% (vol/vol) Tween 20 at a single concentration of 50 μM.

Labeling of Cells with Fluorescent Ligands

In experiments where dextran was used as a lysosomal marker, dextran was added directly to cell cultures to a final concentration of 50 μg/ml 16–18 h preceding the experiment while cells were maintained in the cell culture incubator. Dextran media was replaced with fresh dextran-free media and returned to the cell culture incubator for 1 h before labeling with Fc to ensure dextran localization in the lysosomal compartment. All other cell incubations were performed at 37°C on a slide warmer in a humidified chamber in 1× medium 1 with ovalbumin (150 mM NaCl, 20 mM HEPES, 1 mM CaCl$_2$, 5 mM KCl, 1 mM MgCl$_2$, 180 mg/ml glucose, and 200 mg/ml ovalbumin) at pH 7.4 (Brown *et al.,* 2000; Wang *et al.,* 2000). Coverslip dishes were equilibrated in several changes of prewarmed medium 1 with ovalbumin before labeled reagents were applied. Labeled Fc was applied at a concentration of 200

Table 1. Binding affinities of the humanized Fcs for human and mouse FcRn at pH 6.0

	Human FcRn				Mouse FcRn			
	Wild-type Fc (nM)		T250Q/M428L Fc (nM)		Wild-type Fc (nM)		T250Q/M428L Fc (nM)	
	K_{d1}	K_{d2}	K_{d1}	K_{d2}	K_{d1}	K_{d2}	K_{d1}	K_{d2}
Texas-Red labeled	100 ± 8 (85)	9 ± 0.3 (15)	7.5 ± 0.6 (92)	2.0 ± 0.2 (8)	10.6 ± 0.7 (93)	4.5 ± 1.7 (7)	2.5 ± 0.4 (96)	0.7 ± 0.2 (4)
Unlabeled	80 ± 3 (87)	17 ± 4 (13)	1.9 ± 0.3 (95)	3 ± 1 (5)	3.2 ± 0.2 (91)	0.5 ± 0.1 (9)	0.4 ± 0.01 (94)	0.2 ± 0.1 (6)

K_d values are mean ± SD as determined in three separate binding experiments, with percent shown in parentheses. The percent values represent the percent population of Fc–FcRn complexes for each K_d value, as determined by the heterogeneous binding model.

μg/ml (4.4 μM) with a labeling time of 10 min unless noted differently in the figure legends. When dextran was used as a marker for fluid phase pinocytosis, it was applied at 250 μg/ml simultaneously with other fluorescent ligands. Labeled transferrin was used at a concentration of 30 μg/ml. In chase experiments, coverslips were briefly rinsed in 1× medium 1 with ovalbumin with fresh buffer applied for the chase interval. After labeling and/or chase, coverslips were placed on ice, rinsed quickly in several changes of ice-cold PBS, and then fixed with cold 4% paraformaldehyde in 1× PBS for 10 min.

Competition Studies. In competition experiments, fluorescent Fc was applied at a concentration of 100 μg/ml and unlabeled Fc at 2 mg/ml (20-fold excess) with a labeling time of 10 min.

Live Cell Chase Experiments. Fc probe was added to buffer-equilibrated coverslips, which were then tightly secured to a prewarmed microscope stage maintained at 37°C and equipped with a reservoir for rinsing and replacing labeling solution with prewarmed medium 1 with ovalbumin. During the 20-min Fc-labeling period, positions of individual FcRn-transfected cells were identified using the 488 laser, and cell positions were recorded for further analysis. Image Z-series were captured immediately after rinse and replacement of labeled probe (time 0) and at subsequent 5-min chase intervals.

Microscopy and Image Processing

Confocal images were captured using an UltraVIEW Spinning Disk Confocal system (Perkin Elmer-Cetus Applied Biosystems, Norwalk, CT) mounted on a Nikon TE2000U inverted microscope (Melville, NY) and equipped with lasers providing excitations at 488, 568, and 647 nm. The system is equipped with a Hamamatsu Orca-ER CCD system (Bridgewater, NJ). Z-series were captured using a 60× NA 1.2 water immersion objective with slice spacing between 0.3–0.5 μm. Images were processed using MetaMorph image processing software (Universal Imaging, West Chester, PA). All system settings were maintained identically for experiments where quantitative comparisons were to be performed. Whenever possible, signal saturation was avoided, and cells with saturated pixels were eliminated from analysis. Images shown in figures were contrast-stretched to enhance the visibility of dim structures, and specific care was taken never to enhance the contrast in such a way that dim objects were deleted from an image. Images to be compared were always contrast-enhanced identically unless noted differently in figure legends.

Quantification of Cellular Fluorescence

For image volumes that were quantified, the fluorescence signal in each image plane was corrected for background by subtracting the median intensity of a 32 × 32-pixel region surrounding each pixel (Maxfield and Dunn, 1990), and then all images of the volume were summed together. A region of interest was drawn around individual transfected or untransfected cells and the average pixel intensity (average gray level) was recorded for each fluorescent probe in the cell.

Statistical Analyses

Regressions were calculated and plotted in KaleidaGraph (Synergy Software, Reading, PA) and statistical tests of significance of regression and analysis of covariance (ANCOVA) were calculated according to Sokal and Rohlf (1995).

RESULTS

Studies of the role of FcRn in Fc internalization were undertaken using HULEC-5A microvascular endothelial cells. Although we found that the HULEC-5A cells used in our studies express endogenous FcRn, as determined via RT-PCR using human-specific primers, the levels of expression

were too low to characterize early events of endocytosis (similar to Ward *et al.*, 2003). To increase the sensitivity of the system we transiently transfected mouse or human GFP-FcRn in a dual expression vector containing both the αFcRn and β2microglobulin subunits, which helped to confirm that both subunits required for normal trafficking would be present in individual GFP-positive transfectants. Transfection efficiency was estimated at 10–20% (data not shown). The presence of untransfected cells adjacent to transfected cells in each experiment provided useful comparisons for the quantitative microscopy studies conducted here. Previous studies have demonstrated that addition of GFP to the carboxy terminus of FcRn does not perturb its characteristic pH-dependent binding to Fc (Tesar *et al.*, 2006).

Trafficking studies were conducted using fluorescently labeled Fc molecules, which we found provided better fluorescent signal than IgG for our assay system. Fluorescent labeling of the WT and two Fc mutants with Texas Red dye showed consistent reproducibility of dye-to-protein ratio between the different Fcs and across multiple labeling reactions.

BIAcore surface plasmon resonance (SPR) data for binding of the various Fc probes to recombinant, soluble hFcRn and mFcRn at pH 6.0 are shown in Table 1 (sensorgrams are shown in Supplementary Data). Consistent with previous reports, affinity of these human Fcs was higher for mouse FcRn than for human FcRn (Zhou *et al.*, 2003; Dall' Acqua *et al.*, 2002). The T250Q/M428L mutant enhanced binding to FcRn relative to WT, whereas the H435A mutant demonstrated no detectable binding, consistent with previous reports (Firan *et al.*, 2001; Hinton *et al.*, 2004) and our previous findings with the corresponding IgGs (Datta-Mannan *et al.*, 2007a; Datta-Mannan *et al.*, 2007b). Fluorescent labeling of Fcs modestly reduced their affinities for FcRn but, importantly, did not alter the rank-order to binding affinities. As in previous reports (Datta-Mannan *et al.*, 2007a,b), we did not detect direct binding of the WT or variant Fcs to human or murine FcRn at concentrations as high as 50 μM at pH 7.4 (sensorgrams in Supplementary Data). However, the relative rates of dissociation of the various Fcs at pH 7.4 mirrored their binding affinities at pH 6.0. In studies in which binding was conducted at pH 6.0 and dissociation subsequently was evaluated at pH 7.4, the dissociation phase half-lives of Fc were slower for mouse FcRn relative to human FcRn and slower for T250Q/M428L Fc relative to WT (sensorgrams are shown in Supplementary Data).

After Short-Term Incubations, Internalized Fcs Colocalize with Human FcRn and Transferrin in Recycling Compartments and not with Lysosomal Dextran

To evaluate the internalization and intracellular trafficking of Fcs, transfected HULEC-5A cells were incubated with
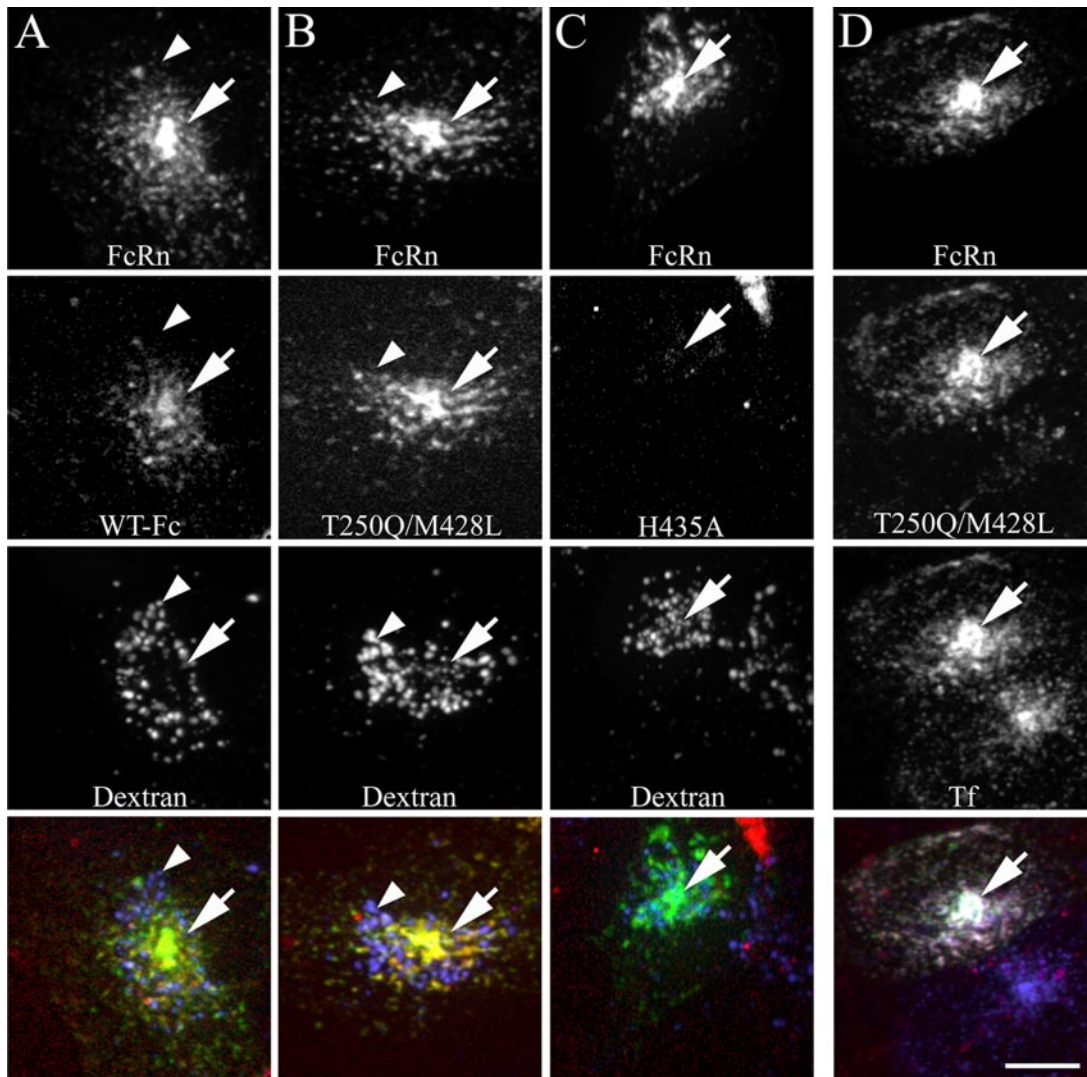
Figure 1. Fc colocalizes with human FcRn and transferrin in recycling compartments and is not present in lysosomes during short-term labeling. Cells expressing human GFP-FcRn were labeled for 20 min with 200 μg/ml TxR-Fc (4.4 μM) at pH 7.4 and then fixed. Cells were either prelabeled with Alexa 647-dextran as a lysosomal marker (50 μg/ml overnight dextran incubation chased to lysosomes for 1 h before addition of Fcs; A–C) or labeled simultaneously with 30 μg/ml Cy5-Tf (D). Projections were made of three-dimensional (3D) image volumes for each fluor and were merged as single images in the bottom row (green, GFP-FcRn; red, Fc; blue, dextran; yellow, colocalization of GFP-FcRn and FC; white (bottom right image only), three color colocalization of GFP-FcRn, Fc, and transferrin). WT Fc (A) and the T250Q/M428L mutant Fc (B) strongly colocalize with human FcRn with prominent fluorescence in the pericentriolar recycling compartment (arrows). Very little fluorescence is observed in the dextran lysosomal compartment (arrowheads). Fluorescent Fc endosomes are very dim in cells labeled with the H435A mutant (C). Cells labeled with Fc and transferrin show extensive colocalization between Fc, transferrin and FcRn (D). Note untransfected cell in D (bottom cell), which labels with transferrin but shows very little Fc internalization. All images from a given fluor were processed and contrast-adjusted in an identical manner, with the exception of the WT Fc images, which were contrast-stretched threefold relative to T250/M428L in order to visualize the overall dimmer labeling, and the H435A images, which were likewise stretched threefold for comparability to the WT Fc images. Scale bar, 10 μm.

TxR-Fcs at pH 7.4 for 20 min, fixed, and imaged by confocal microscopy. To provide a marker of lysosomes, cells were previously incubated in Alexa 647-dextran overnight and then in unlabeled medium for an hour before addition of TxR-Fc. Figure 1 shows projected images of cells incubated with the WT Fc (column A), the high-affinity T250Q/M428L mutant (column B) and the nonbinding H435A mutant (C). In all three cases, GFP-FcRn is distributed in punctate compartments and concentrated in a pericentriolar compartment (indicated with arrows). The two Fcs with confirmed binding affinity for FcRn (WT and T250Q/M428L) were both internalized into the FcRn-containing compartments, colo-

calizing with FcRn almost completely. Consistent with their recycling itineraries, little if any FcRn or internalized Fc is found in lysosomes, as labeled with internalized dextran (arrowheads). In contrast, minimal Fc fluorescence was observed in cells incubated with TxR-H435A (column C). Because the fluorescence of this conjugate is similar to that of the other two probes, the reduced labeling appears to reflect less internalization, a surprising result given that internalization is thought to occur via fluid-phase bulk internalization (Junghans and Anderson, 1996; Ghetie and Ward 2000, 2002).

Similar to other studies of cells expressing a C-terminal GFP-FcRn fusion protein (Ober *et al.*, 2001, 2004a,b; Ward *et*
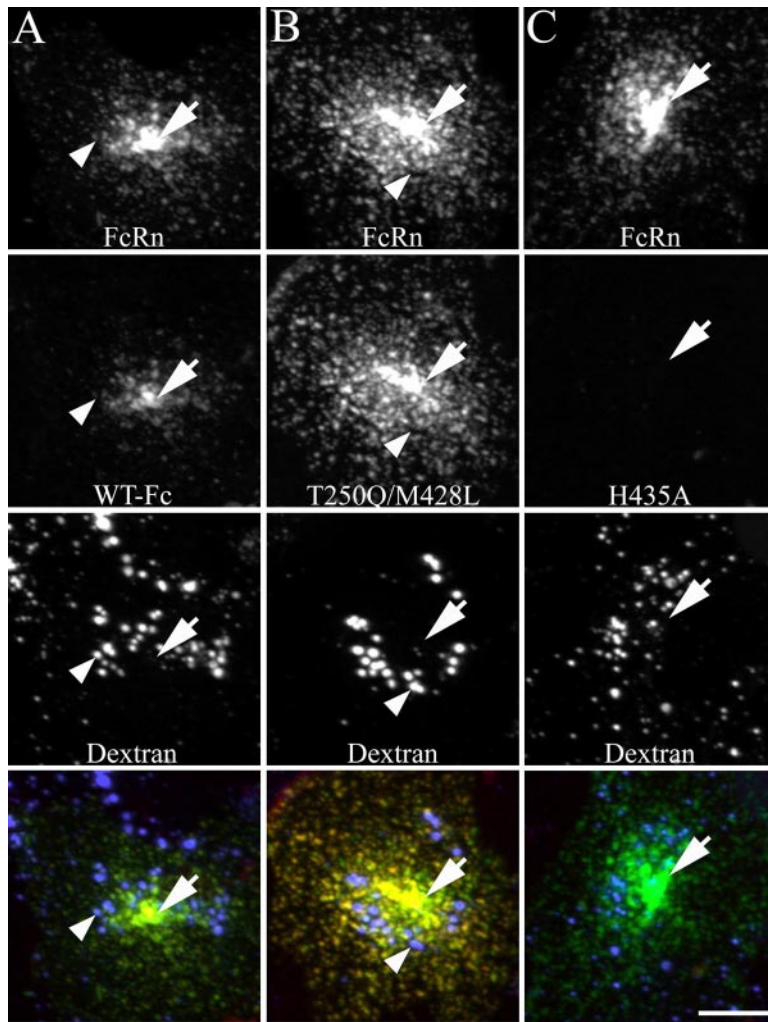
Figure 2. Fc internalization and distribution in cells transfected with mouse FcRn is comparable to those transfected with human FcRn. Cells expressing mouse GFP-FcRn were labeled for 20 min with 200 μg/ml TxR-Fc at pH 7.4 and then fixed. Cells were prelabeled with Alexa 647-dextran as a lysosomal marker (50 μg/ml overnight dextran incubation chased to lysosomes for 1 h before addition of Fcs). Projections were made of 3D image volumes for each fluor and were merged as single images in the bottom row (green, GFP-FcRn; red, Fc; blue, dextran; yellow, colocalization of GFP-FcRn and Fc). WT Fc (A) and the T250Q/M428L mutant Fc (B) colocalize with mouse FcRn in the PRC (arrows) and early endosomes but is not present in the lysosomes (arrowheads). Minimal internalization of the H435A mutant is observed (C). All images were contrast-adjusted in an identical manner to compare relative fluorescent intensities. All images from a given fluor were processed and contrast-adjusted in an identical manner. Note that the WT Fc image (A) is brighter and more readily visualized than the comparable image in Figure 1A of Fc internalization by a cell transfected with human FcRn, which required contrast stretching for visualization. Scale bar, 10 μm.

al., 2005; Tesar *et al.,* 2006), GFP-FcRn is largely distributed in intracellular compartments and is nearly undetectable at the cell surface. Because previous studies (Ward *et al.,* 2005) have associated FcRn with the endocytic recycling pathway, the distribution of Fc and FcRn was compared with that of transferrin, which labels the entire endocytic recycling pathway. Cells in column D were simultaneously labeled for 20 min with fluorescent TxR-T250Q/M428L and Cy5-transferrin. Nearly complete colocalization is observed between FcRn, transferrin, and Fc, as reflected in the combined white color of the endosomes in the color-merged image of the transfected cell. This colocalization confirms that FcRn and internalized Fc are predominantly localized in endosomes of the recycling pathway and largely accumulated in a well-defined pericentriolar recycling compartment (PRC), but also are apparent in endosomes dispersed throughout the cell.

Although the fluorescence of the WT and T250Q/M428L conjugates are similar, the fluorescence intensity of cells incubated with the WT is consistently lower than that of cells incubated with the T250Q/M428L mutant under similar labeling conditions. In Figure 1, it was necessary to increase the brightness of WT Fc threefold relative to that of the T250Q/M428L mutant, in order to visualize labeled structures and demonstrate colocalization between Fc and FcRn. (Note that the brightness of the brightness of the TxR-H435A fluorescence shown in column C was likewise increased threefold for comparability with TxR-WT.)

Cells Expressing Mouse GFP-FcRn Traffic Human Fc Similarly to Cells Expressing Human GFP-FcRn, but with More Robust Fc Internalization

When similar short-term incubations are performed using cells transfected with mouse GFP-FcRn, patterns of colocalization between labeled Fc and FcRn are very similar to those observed in cells expressing human GFP-FcRn. As shown in Figure 2, both WT Fc (column A) and T250Q/M428L (column B) closely colocalize with FcRn in the recycling compartment (arrows) and in dispersed endosomes, but both are absent from lysosomes (arrowheads). As was found for cells expressing human FcRn, minimal internalization of the H435A mutant was observed in cells expressing mouse GFP-FcRn (column C).

The endosomal fluorescence of internalized WT Fc and T250Q/M428L is consistently brighter and more easily distinguished in mouse FcRn transfectants (Figure 2) than in human FcRn transfectants (Figure 1) during equivalent short labeling periods. (Note that although the low intensity of the WT image relative to T250Q/M428L required threefold multiplication for visualization in Figure 1, WT and T250Q/M428L are adjusted identically in Figure 2).

Indeed, the intensities of endosomal fluorescence in the studies described above correlate overall with the relative affinities of each of the Fc-FcRn interactions, as listed in Table 1. The strongest endosomal fluorescence is observed

Figure 3. Fc recycles from cells transfected with mouse GFP-FcRn. Coverslip dishes of cells transfected with mouse GFP-FcRn were equilibrated in medium 1 with ovalbumin and secured to the microscope stage maintained at 37°C. Cells were labeled for 15 min on the microscope stage with prewarmed TxR-WT (200 µg/ml) and then rinsed in a large volume of prewarmed buffer. Live image stacks were collected at time 0 (A), 10 (B), and 30 min (C), and projections were made of 3D volumes. Rapid movement of fluorescent endosomes was observed throughout the course of the experiment, indicating adequate maintenance of appropriate temperature and pH conditions. Scale bar, 10 µm.
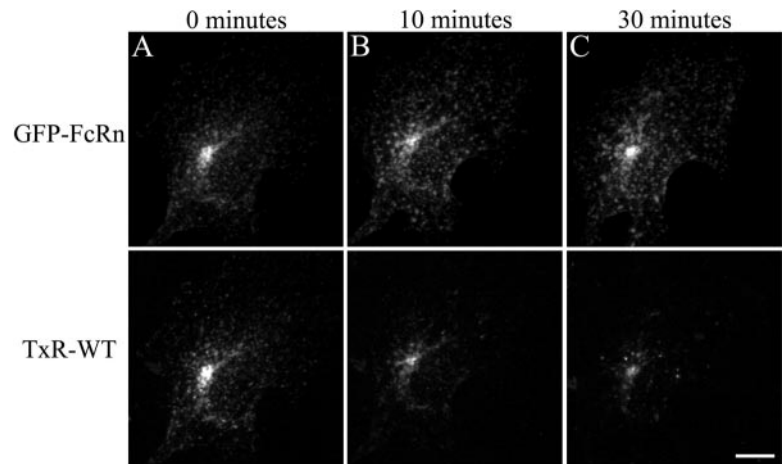
for mouse FcRn transfectants incubated with the T250Q/M428L mutant, and much weaker endosomal fluorescence is found for human FcRn transfectants incubated with WT Fc and the weakest fluorescence observed in either transfectant incubated with the H435A mutant. The correlation between binding affinity and Fc internalization is inconsistent with a simple model of fluid-phase endocytosis, a topic we address later.

Because the mouse FcRn transfection system demonstrates greater sensitivity than the human system for visualization by confocal microscopy, yet shows equivalent patterns of labeling, subsequent experiments were performed primarily in the mouse system, enabling studies with even shorter incubation periods.

Fc Recycles from GFP-FcRn Transfected Cells

To observe the trafficking of Fcs in real time, cells expressing mouse GFP-FcRn were incubated with TxR-Fc at pH 7.4 for 15 min on a heated microscope stage. At the end of the incubation, the labeling solution was replaced with buffer lacking fluorescent probes, and confocal image volumes were collected at successive chase intervals. As shown in Figure 3A, immediately after the labeling, endosomes containing both FcRn and Fc are abundantly distributed throughout the cytoplasm, as well as strongly concentrated in the PRC. After a 10-min chase (column B), there is a significantly less Fc in the cell, with a large drop in fluorescence in the PRC. Fc-containing endosomes observed moving through the cytoplasm are fewer and much dimmer. Fc fluorescence decreases further after 30 min of chase (column C). Time-series studies demonstrate that Fc effluxes from compartments of the recycling pathway, as identified by the presence of GFP-FcRn. However, over this same period of time Fc modestly accumulates in compartments lacking GFP-FcRn, consistent with direction of a fraction of the residual cell-associated Fc to compartments of the degradative pathway. As expected, GFP-FcRn fluorescence remains constant throughout the chase. Consistent with the idea that Fc recycling is facilitated by FcRn, no recycling of internalized Fc was observed in nontransfected cells (data not shown).

Expression of GFP-FcRn Increases Internalization of Fc, but not Fluid-Phase Probes

As mentioned above, we find that the amount of Fc internalization correlates closely with the affinity of each Fc for each FcRn. This is a surprising result, given that internaliza-

tion is thought to occur via fluid-phase internalization, with FcRn-Fc interactions occurring only in the acidic lumens of endosomes. We also noticed that cells expressing GFP-FcRn internalized significantly more Fc than neighboring, nontransfected cells. Although this suggests that Fc is internalized via binding to the FcRn, it is also possible that transfection and/or expression of GFP-FcRn somehow alters the rates of fluid-phase endocytosis. To determine whether expression of GFP-FcRn increased fluid-phase endocytosis, transfected cells were incubated simultaneously with both TxR-Fc and Alexa 647-dextran, a fluid-phase probe, for 10 min.

Figure 4 shows the results of studies of transfected HULEC-5A (column A) and MDCK cells (column B). In both cell types, significant Fc internalization is observed only in transfected cells, with minimal Fc fluorescence detected in untransfected cells. In contrast, dextran appears to be present at equivalent levels in both transfected and untransfected cells, demonstrating that the increased Fc internalization found in transfected GFP-FcRn does not reflect higher rates of fluid-phase endocytosis in transfected cells.

In addition to a relative lack of Fc internalization by untransfected cells during short labeling experiments, it was visually apparent that the quantity of Fc internalized by individual transfected cells was related to their level of GFP-FcRn expression. Cells with low levels of GFP-FcRn expression showed dim Fc labeling, whereas robust internalization was found in cells expressing high levels of GFP-FcRn. To quantify this relationship, we measured total fluorescence levels of GFP-FcRn, Fc, and dextran in individual cells after 10-min incubations in both Fc and dextran. In Figure 4C, GFP-FcRn fluorescence is plotted against the fluorescence intensity of WT Fc and dextran for a population of cells. Regression analysis demonstrated a highly significant linear relationship between FcRn expression level and internalized Fc fluorescence ($p = 7.9 \times 10^{-11}$). For reasons we do not understand, the regression of dextran internalization was marginally significant ($p = 0.0283$), but the relationship was much weaker; dextran internalization increased by <50% over the observed range of FcRn expression levels, whereas Fc internalization increased more than fivefold, a significantly higher rate (ANCOVA, $p = 4.5 \times 10^{-8}$). This disproportionate increase in internalization of Fc relative to dextran indicates that FcRn mediates internalization of Fc, increasing its concentration in endosomes beyond the levels that would result from fluid-phase endocytosis. The role of FcRn in concentrative endocytosis of Fc
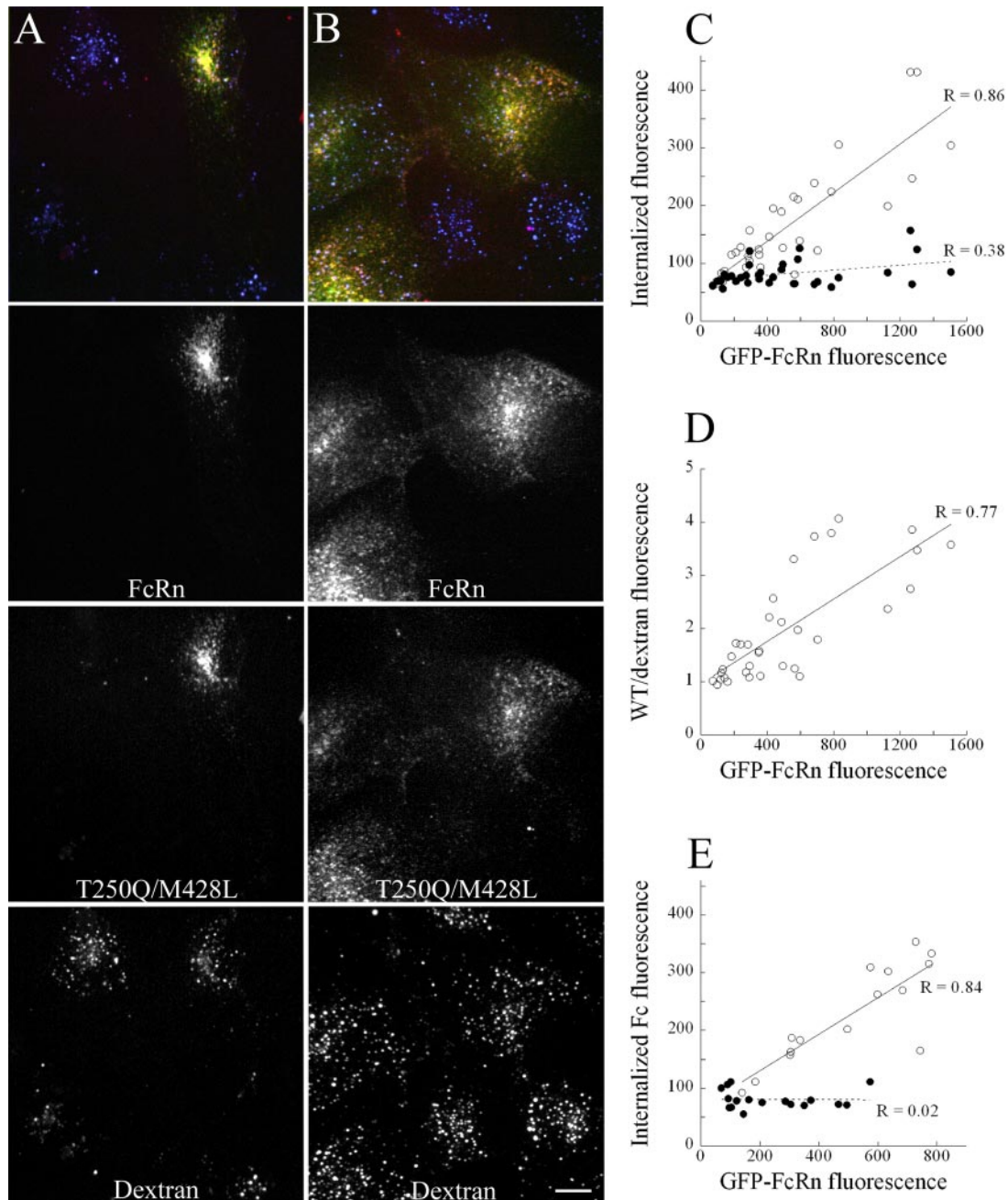
Figure 4. HULEC-5A (A) and MDCK (B) cells were transfected with mouse GFP-FcRn and incubated for 10 min in mixture of 200 μg/ml TxR-Fc (T250Q/M428L) and 250 μg/ml Alexa 647-dextran and then fixed. After this short incubation, Fc internalization is visible only in the transfected, but not the untransfected cells in either cell line. In contrast, dextran internalization by fluid phase pinocytosis appears comparable in both transfected and nontransfected cells. Scale bar, 10 μm. (C–E) Quantifications of Fc and dextran internalization by HULEC5A cells transfected with mouse FcRn. Cells were incubated for 10 min with 200 μg/ml TxR-WT and 250 μg/ml Alexa 647-dextran and then fixed. Total cell fluorescence was recorded for each fluor from projections of 3D volumes of 35 cells. Although dextran internalization remains constant between cells (C, ●), Fc internalization (C, ○) and the ratio of Fc/dextran (D) increase in a linear manner with increasing expression of FcRn. E. Mouse FcRn-transfected cells were labeled for 20 min with 200 μg/ml either TxR-T250Q/M428L or TxR-H435A. Cellular fluorescence of the T250Q/M428L (○, n = 15) but not the H435A mutant (●, n = 17) increases with GFP-FcRn fluorescence.

is demonstrated in Figure 4D, where we have presented the same data in terms of Fc-to-dextran ratios, showing that the enrichment of Fc internalization relative to dextran increases with the level of GFP-FcRn expression (regression analysis, $p = 7.3 \times 10^{-8}$). (Note that regression and ANCOVA analyses are summarized in Table 2).

Similar results were obtained in studies of cells incubated for 10 min with fluorescently labeled T250Q/M428L. As with the WT Fc, internalization of T250Q/M428L increased linearly with FcRn expression ($p = 8.6 \times 10^{-5}$). In contrast, internalization of the nonbinding Fc mutant H435A was significantly decreased (ANCOVA, $p = 5.6 \times 10^{-5}$) and was

Table 2. Summary of statistical analyses of internalization data

Graph	Function	Regression equation	Coefficient of determination (R^2)	Probability of random relationship	Sample size	ANCOVA comparison of slopes probability
4 C	Fc vs. FcRn	$y = 0.210x + 54.4$	0.738	$p = 7.9 \times 10^{-11}$	35	$p = 4.5 \times 10^{-8}$
	Dextran vs. FcRn	$y = 0.0116x + 70.7$	0.142	$p = 0.0283$	35	
4 D	Fc/dextran vs. FcRn	$y = 0.002x + 0.962$	0.601	$p = 7.3 \times 10^{-8}$	35	
4 E	T250Q/M428L vs. FcRn	$y = 0.316x + 67.0$	0.707	$p = 8.6 \times 10^{-5}$	15	$p = 0.000056$
	H435A vs. FcRn	$y = -.0022x + 81.2$	0.005	$p = 0.9333$	17	
5 I	Fc vs. FcRn	$y = 0.00152x + 55.5$	0.443	$p = 0.0005$	23	$p = 0.000078$
	Fc vs. FcRn − competition	$y = 0.0035x + 53.7$	0.087	$p = 0.206$	20	
5 J	T250Q/M428L vs. FcRn	$y = 0.202x + 63.9$	0.608	$p = 1.15 \times 10^{-5}$	23	$p = 0.000042$
	T250Q/M428L vs. FcRn competition	$y = 0.025x + 65.1$	0.311	$p = 0.00860$	21	
5 K	Fc vs. FcRn	$y = 0.133x + 44.9$	0.740	$p = 5.67 \times 10^{-5}$	21	$p = 0.300$
	Fc vs. FcRn H435A competition	$y = 0.117x + 36.6$	0.870	$p = 5.16 \times 10^{-13}$	28	
5 L	T250Q/M428L vs. FcRn	$y = 0.115x + 83.6$	0.280	$p = 0.0079$	24	$p = 0.076$
	T250Q/M428L vs. FcRn, H435A competition	$y = 0.195x + 48.3$	0.775	$p = 6.69 \times 10^{-9}$	25	
7 E	Fc vs. FcRn	$y = 0.196x + 52.8$	0.894	$p = 3.51 \times 10^{-13}$	26	$p = 6.70 \times 10^{-15}$
	Dextran vs. FcRn	$y = 0.023x + 71.1$	0.312	$p = 0.003$	26	
7 F	Fc vs. FcRn	$y = 0.238x + 33.6$	0.762	$p = 7.0 \times 10^{-7}$	21	$p = 1.25 \times 10^{-7}$
	Dextran vs. FcRn	$y = 0.014x + 78.0$	0.040	$p = 0.384$	21	
8 E	Fc vs. FcRn	$y = 0.078x + 65.6$	0.506	$p = 1.4 \times 10^{-4}$	23	

unrelated to FcRn expression level (p = 0.9333; Figure 4E). The correlation between Fc internalization and FcRn level was observed in studies conducted on more than 15 different occasions.

Fc Internalization Is Blocked by Competition with Binding Fcs

Although internalization of Fc is thought to be mediated by fluid-phase endocytosis, several aspects of our results indicate receptor-mediated internalization through interactions with FcRn. First, we find that Fc internalization correlates closely with the affinity of each Fc for FcRn. Second, we find that significant Fc internalization is limited to cells expressing FcRn and that the amount of internalization scales proportionally with the level of expression of FcRn. Finally, we find that the internalization of Fc is enriched relative to that of a fluid-phase probe and that the enrichment increases with the level of FcRn expression. Taken together these results suggest that Fc is internalized via binding to the FcRn. To directly test the specificity of internalization, internalization studies were conducted in the presence or absence of a 20-fold excess of unlabeled T250Q/M428L, which would be expected to block FcRn receptor–mediated internalization, but have no effect on fluid-phase internalization of Fc.

Figure 5, A and B, shows examples of transfected HULEC-5A cells incubated for 10 min with 100 μg/ml TxR-T250Q/M428L with or without a 20-fold excess (2 mg/ml) of unlabeled T250Q/M428L. Figure 5, C and D, shows cells from a comparable experiment where a similar 20-fold excess of the nonbinding H435A Fc was used as competitor. These studies clearly demonstrate that internalization of TxR-T250Q/M428L is completely blocked by competition with unlabeled T250Q/M428L, but not H435A Fc. Similar studies show that internalization of WT Fc was likewise blocked by competition with unlabeled T250Q/M428L (Figure 5, E and F), but not H435A Fc (Figure 5, G and H).

Figure 5, I–L, shows the results of quantifying these results to determine the relationship between Fc internalization and GFP-FcRn expression level. Similar to the studies of Figure 4, internalization of WT Fc (Figure 5I) and T250Q/M428L (Figure 5J) linearly increases with the level of expression of GFP-FcRn for cells incubated with fluorescent probes alone (regression analysis, p = 0.005 and 1.15×10^{-5}, respectively). Internalization of both probes was reduced by competition with unlabeled Fc; inclusion of 20-fold excess of unlabeled T250Q/M428L in the incubation medium significantly decreased internalization of both WT (ANCOVA, p = 7.8×10^{-5}) and T250Q/M428L (ANCOVA, p = 4.2×10^{-5}). However, competition with the nonbinding H435A mutant had no effect on internalization of either WT (Figure 5K) or T250Q/M428L (Figure 5L; ANCOVA, p = 0.3 and 0.076, respectively). These studies, demonstrating that internalization of fluorescent Fcs is blocked by competition with a binding mutant, but not by a nonbinding mutant, strongly indicate that internalization of Fc is mediated by binding to GFP-FcRn. Competition studies were conducted on three separate studies, all with the same results.

Internalization of Human Fc Is Mediated by Human FcRn in Transfected HULEC-5A Cells

Because the high-affinity between mouse FcRn and human Fc provides stronger fluorescence in endosomes, most of our studies have utilized this system. However, it is possible that the FcRn-mediated internalization of Fc that we observe in this system reflects some kind of unnatural interaction between these two molecules. To determine whether the human FcRn can mediate internalization of human Fc, HULEC-5A cells expressing human GFP-FcRn were incubated for 20 min with both human Fc and dextran. Figure 6A shows a field containing three cells, as indicated by the internalization of fluorescent dextran, but only the cell expressing GFP-FcRn has internalized significant amounts of TxR- T250Q/M428L. Similarly, Figure 6B shows a field of
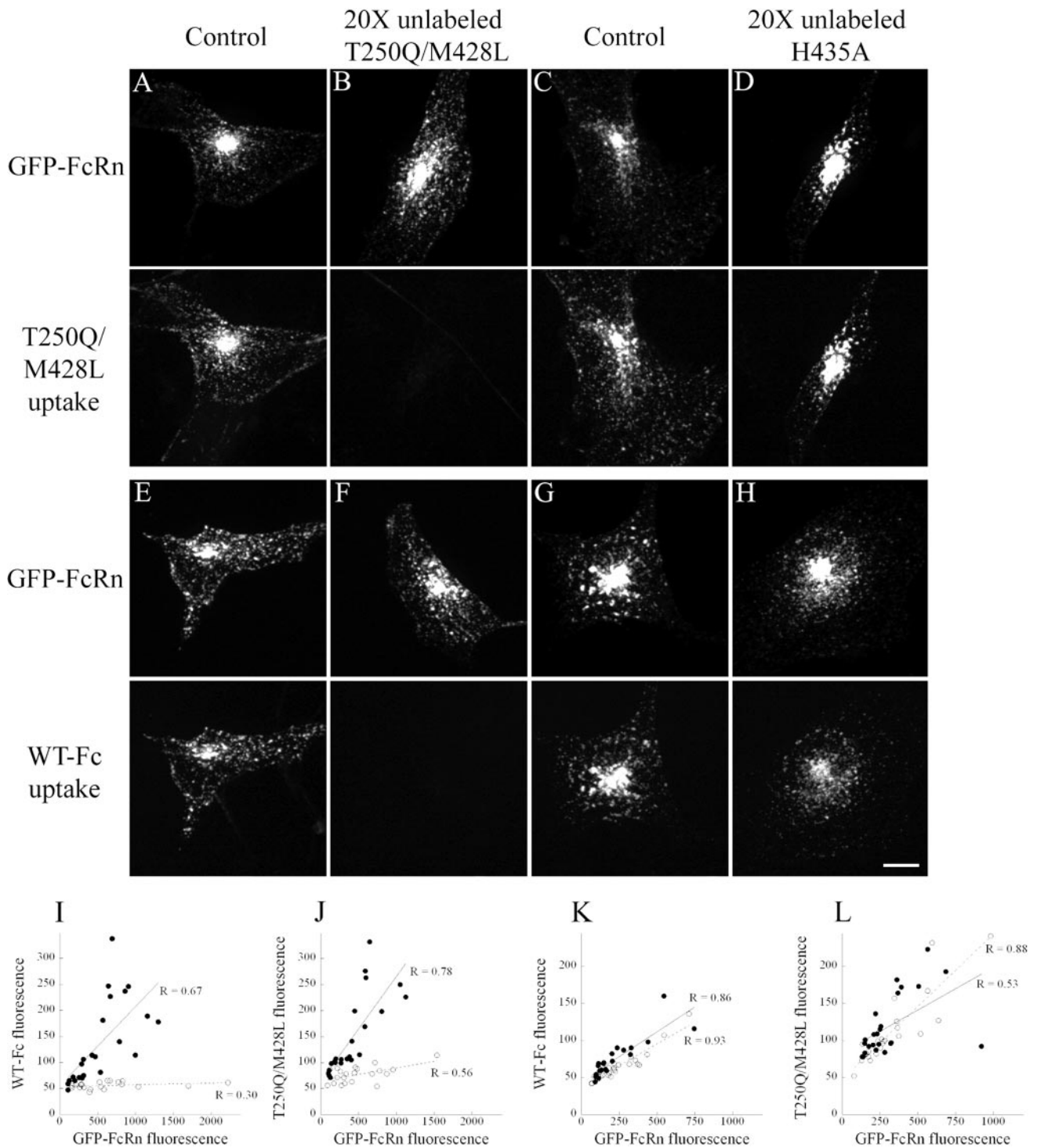
Figure 5. Internalization of fluorescently labeled Fc can be competed by a 20-fold excess of unlabeled FcRn-binding probe, but not nonbinding probe. Mouse FcRn-transfected cells were labeled for 10 min with 100 μg/ml TxR-T250Q/M428L (A–D) or TxR-WT (E–H) and then fixed. Cells in B and F were coincubated with 2 mg/ml unlabeled T250Q/M428L and in D and H were coincubated with 2 mg/ml unlabeled H435A and then fixed. In each of the four experiments, T250Q/M428L and WT controls demonstrated colocalization of the GFP-FcRn and Fc compartments (A, C, E, and G). When either Fc was coincubated with a 20-fold excess of unlabeled T250Q/M428L, Fc fluorescence levels were profoundly reduced (B and F), but little decrease in fluorescent signal was noted when a 20-fold excess of unlabeled H435A was used for the coincubation (D and H). Scale bar, 10 μm. (I–L) Quantifications of competition studies. For each of the conditions above, total cell fluorescence was recorded for each fluor from projections of 3D volumes. Cells incubated with TxR-WT (I) along with unlabeled T250Q/M428L (○, n = 20) showed a clear decrease in internalization of labeled probe relative to noncompeted cells (●, n = 23). Cells incubated with TxR-T250Q/M428L (J) along with unlabeled T250Q/M428L (○, n = 21) showed a clear decrease in internalization of labeled probe relative to noncompeted cells (●, n = 23). No differences in internalization were observed in similar cell populations incubated with TxR-WT (K) with (○, n = 28) or without (●, n = 21) unlabeled H435A. No differences in internalization were observed in similar cell populations incubated with TxR-T250Q/M428L (L) with (○, n = 25) or without (●, n = 24) unlabeled H435A.
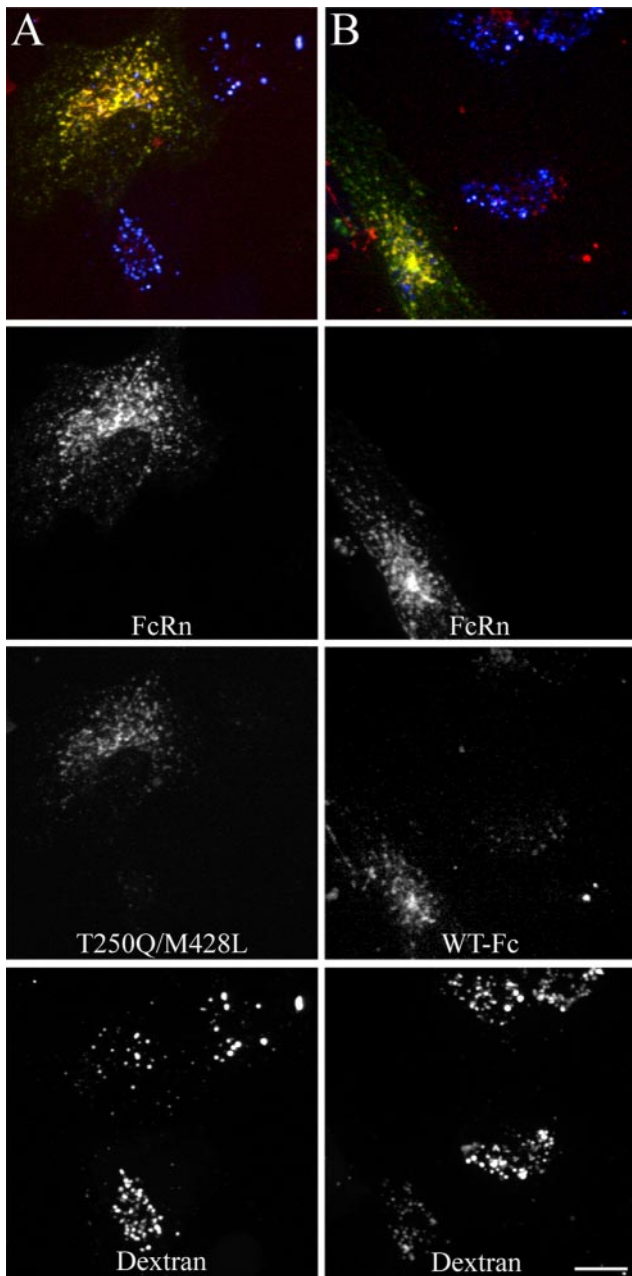
Figure 6. HULEC-5A cells were transfected with human GFP-FcRn and incubated for 20 min in mixture of 200 μg/ml TxR-Fc and 250 μg/ml Alexa 647-dextran and then fixed. After this short incubation, internalization of TxR-T250Q/M428L (A) is visible only in the transfected, but not the untransfected cells. Despite the lower affinity of the TxR-WT Fc (B), internalization was again much more apparent in cells transfected with GFP-FcRn. In both cases, dextran internalization is comparable in transfected and nontransfected cells. Scale bar, 10 μm.

three or four cells, as indicated by dextran internalization, but only the cell expressing GFP-FcRn has internalized a significant amount of WT Fc. These results, which were repeated in seven separate studies, indicate that internalization of human Fc is mediated by human FcRn. This conclusion is also supported by the data shown in Figure 1, which show that the nonbinding H435A mutant Fc is minimally internalized, relative to either the WT or T250Q/M428L mutant.

Internalization of Fc Is Not Significantly Enhanced in Cells Incubated at pH 6.0

Previous studies have demonstrated that the amount of cell-associated Fc/IgG is profoundly increased in cells incubated at acidic pH (Praetor *et al.,* 1999; McCarthy *et al.,* 2000; Yoshida *et al.,* 2004; Stirling *et al.,* 2005; Tesar *et al.,* 2006), a condition where the binding affinity of Fc for FcRn is enhanced. However, the extended incubations (1–2 h) used in these previous studies admit the possibility that some of the increased cell-associated Fc may result from inhibited recycling of Fc at acidic pH, rather than augmented internalization, because an acidic extracellular pH would effectively block release of IgG from recycled FcRn-IgG complexes. To evaluate whether Fc internalization is enhanced at a lower pH, short-term internalization studies were conducted at both pH 6.0 and 7.4. Cells transfected with mouse FcRn were labeled simultaneously with Alexa 647-dextran and either TxR-WT or TxR-T250Q/M428L for 10 min after equilibration at either pH 7.4 or 6.0. Visual inspection of cells did not suggest substantial differences in internalization of either Fc or dextran (Figure 7). As in our previous studies, Fc internalization was restricted to transfected cells at both pH 6.0 and 7.4.

Quantification of total fluorescence demonstrates that Fc internalization at both pH 6.0 and pH 7.4 (Figure 7, E and F, respectively) is linearly related to the level of FcRn expression (p = 3.5×10^{-13} and 7×10^{-7}, respectively). Dextran internalization was unrelated to FcRn expression at pH 7.4 (p = 0.384). At pH 6.0, dextran internalization was positively related to FcRn expression (p = 0.003), but only slightly; dextran internalization increased by <50% over the observed range of FcRn expression levels, whereas Fc internalization increased more than fourfold, a significantly higher rate (ANCOVA, p = 6.7×10^{-15}). Similar results were obtained in multiple samples collected in two separate studies.

The fact that dextran internalization was unaffected by pH indicates that the similar levels of Fc internalization observed at pH 6.0 and 7.4 do not reflect confounding effects of pH on fluid-phase endocytosis. Although the similar slopes of Fc internalization shown in Figure 7, E and F, might be interpreted to suggest similar internalization rates at the two pHs, the two curves cannot be quantitatively compared. First, incubation of the cells at pH 6.0 visibly stressed the cells. Second, an extracellular pH of 6.0 might be expected to affect the rates of membrane internalization and would be likely to affect rates of membrane recycling, which would indirectly impact Fc internalization by altering the ratio of internal-to-surface FcRn. Nonetheless, these studies indicate that FcRn-mediated internalization of Fc was not substantially affected by the pH of the extracellular medium.

Internalization of Fc Is Not Significantly Affected by Endosome Alkalinization

The finding that FcRn-mediated Fc internalization was not significantly enhanced in cells incubated in a pH 6.0 medium compared with a pH 7.4 medium is surprising given the fact that SPR studies demonstrate a significantly higher affinity of Fc for FcRn at acidic pH (Table 1). One possible explanation for this observation is that even in a neutral culture medium, Fc may interact with FcRn in an acidic local environment during internalization.

Binding of Fc to FcRn expressed in cells incubated at pH 7.4 may result from acidification of the local environment of the FcRn at the cell surface, as can result from the presence of charged sugars on the extracellular face of the plasma membrane (Kovbasnjuk and Spring, 2000) or via the activity
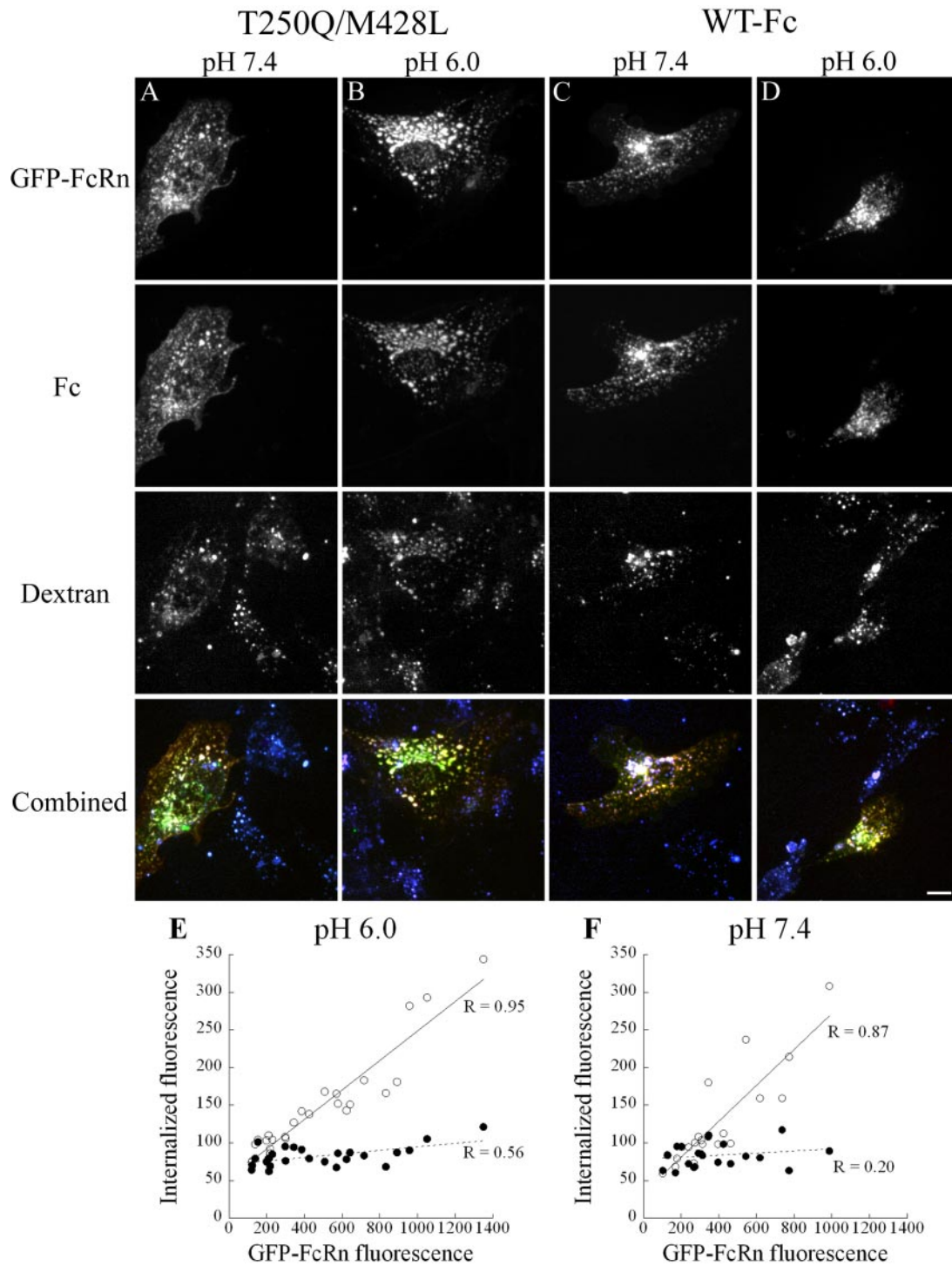
Figure 7. Fc internalization is similar at pH 6.0 and 7.4. Mouse FcRn-transfected cells were equilibrated for 10 min at pH 7.4 or 6.0 and then labeled for 10 min with 200 μg/ml TxR-WT or TxR-T250Q/M428L and 250 μg/ml Alexa 647-dextran at pH 6.0 or 7.4 and then fixed. (A and B) T250Q/M428L after incubation at pH 7.4 (A) or 6.0 (B). (C and D) WT after incubation at pH 7.4 (C) or 6.0 (D). No differences are noted in relative internalization of Fc (row 2) or dextran (row 3) at either pH. Merged images (row 4) show comparable colocalization of Fc with FcRn at either pH. Scale bar, 10 μm. (E and F) Quantification of the effect of incubation pH on Fc internalization. For each of the conditions above, total cell fluorescence was recorded for each fluor from projections of 3D volumes. Internalization of TxR-WT ($\bigcirc$), but not dextran ($\bullet$) increases proportionally to FcRn at both pH 6.0 (E, n = 26) and pH 7.4 (F, n = 21).

of sodium-proton exchangers in the plasma membrane (Maouyo *et al.*, 2000). However, in studies of cells incubated with fluorescent Fc at 4°C, we failed to see evidence of binding of Fc to the surface of cells (data not shown).

Alternatively, FcRn-mediated internalization of Fc may be mediated by uptake of Fc into acidic endosomes. To test the role of acidic endosomes in FcRn-mediated internalization of Fc, we evaluated internalization of Fc by cells treated with
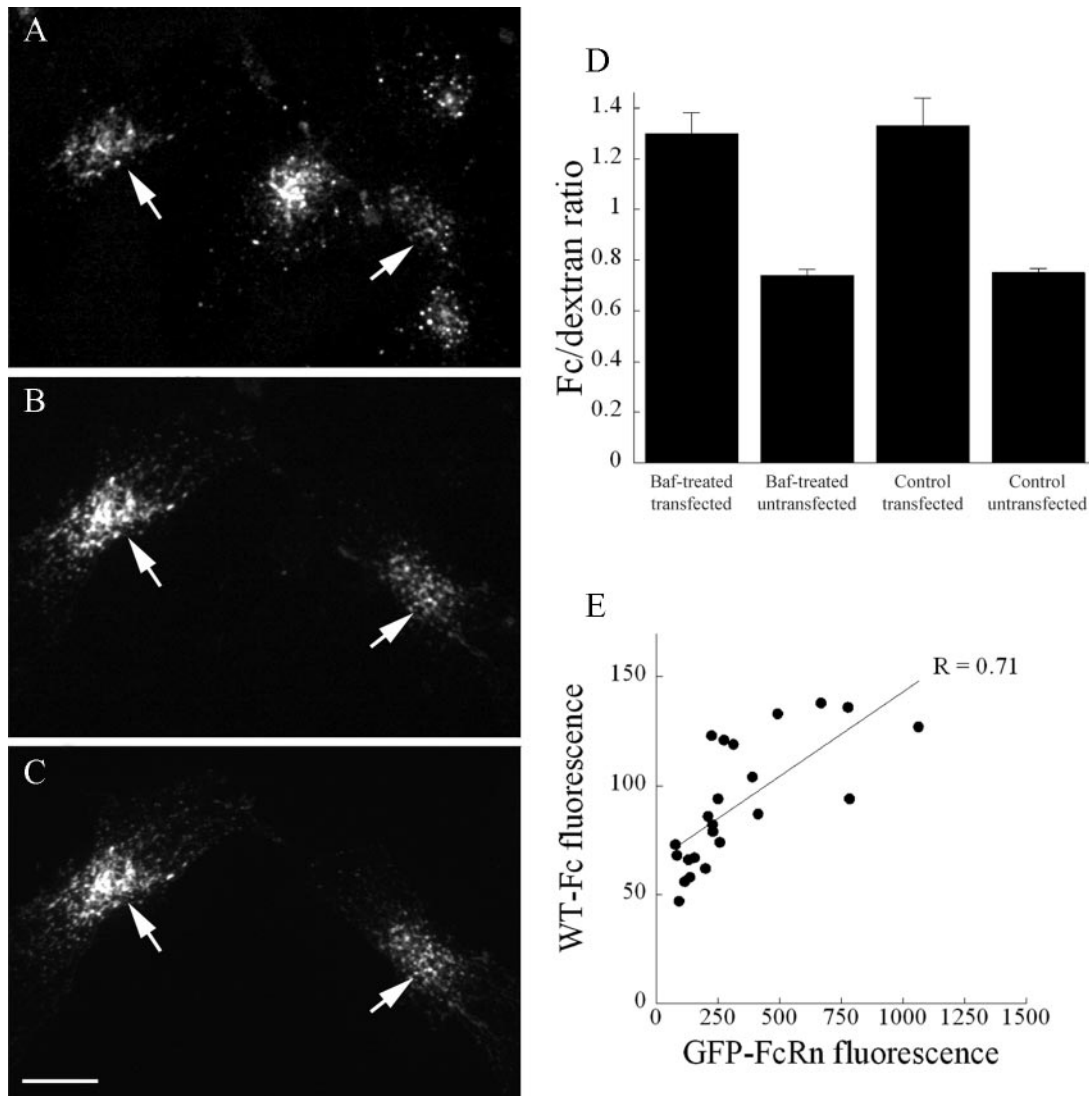
Figure 8. FcRn-mediated internalization of Fc is not significantly affected by endosome alkalinization. Mouse FcRn-transfected HULEC-5A endothelial cells were preincubated for 15 min with 1 μM bafilomycin and then incubated for 15 min with TxR-WT and Cy5-dextran in the continued presence of bafilomycin. Cells were then fixed for analysis. (A–C) Fluorescence micrographs of bafilomycin-treated cells. (A) Internalization of Cy5-dextran by five cells in the field, (B) Expression of GFP-FcRn by two cells in the field. (C) Internalization of TxR-WT by the two GFP-FcRn-expressing cells. (D) Quantification of internalization of Fc and dextran. For each of the conditions above, total cell fluorescence was quantified for each fluor from projections of 3D volumes. Expression of GFP-FcRn enriches internalization of Fc relative to dextran in both bafilomycin-treated (n = 30, 25) and untreated cells (n = 31, 27). (E) Internalization of Fc increases linearly with expression of GFP-FcRn in bafilomycin-treated cells (n = 23). Scale bar, 10 μm.

bafilomycin, an inhibitor of the endosomal proton ATPase, which increases the pH of early endosomes from 5.8 to 6.0 to between 6.6 and 7.0 (Johnson *et al.,* 1993; van Weert *et al.,* 1995; Presley *et al.,* 1993). HULEC-5A endothelial cells were preincubated for 15 min with 1 μM bafilomycin and then incubated for 15 min with TxR-WT and Cy5-dextran in the continued presence of bafilomycin. The alkalinizing effect of bafilomycin in these studies was verified in separate studies of cells labeled with a pH-sensitive transferrin (data not shown).

The results of these studies, summarized in Figure 8, show that bafilomycin has no effect on FcRn-mediated internalization of Fc. Fluorescence micrographs of a field of bafilomycin-treated cells are shown in Figures 8, A–C. Panel A shows internalization of Cy5-dextran by five cells in this field. However, internalization of TxR-WT (B) is apparent only in

the cells expressing GFP-FcRn (C), indicated by arrows. Figure 8D shows quantifications of Fc and dextran internalization by the cells in this study. In both bafilomycin-treated and control cells, expression of GFP-FcRn significantly enriched internalization of Fc relative to the fluid-phase dextran ($p = 2.5 \times 10^{-7}$, $p = 9.4 \times 10^{-6}$, respectively). Indeed, the FcRn-mediated enrichment of Fc internalization in bafilomycin treated cells was indistinguishable from that of untreated cells ($p = 0.84$, ANCOVA).

That bafilomycin has no effect on FcRn-mediated internalization of Fc is also indicated by the fact that we find the same relationship between Fc internalization and FcRn expression in bafilomycin-treated cells as we have previously observed in untreated cells (Figure 8E). Although untransfected cells internalized only background levels of Fc (mean of 59 Gy levels, n = 25), cells expressing GFP-FcRn internal-

ized more Fc in proportion to the level of GFP-FcRn expression (p = 1.4×10^{-4}). Statistical comparison of this regression with that of untreated cells shows that the relationship between Fc internalization and GFP-FcRn expression is not significantly affected by bafilomycin treatment (p = 0.31, ANCOVA). Similar results were obtained in studies of cells treated with 40 mM methylamine, which likewise alkalinizes endosomes (Dunn *et al.,* 1994; Wang *et al.,* 2000). These studies, which were repeated on five separate occasions, with the same results, indicate that FcRn-mediated internalization of Fc occurs even under conditions in which endosome acidification is impaired.

DISCUSSION

Because FcRn has a weak affinity for IgG or Fc molecules at neutral pH, FcRn-receptor mediated endocytosis has been believed to be significant only in cells expressing FcRn on the plasma membrane surface exposed to an acidic environment, such as in intestinal epithelia (Rodewald, 1976, 1980; Wallace and Rees, 1980; Rodewald and Kraehenbuhl, 1984). Internalization of Fc or IgG molecules from neutral extracellular spaces is generally thought to occur via fluid-phase internalization, with subsequent binding to FcRn in acidic endosomes required for recycling (Rodewald and Kraehenbuhl, 1984; Junghans and Anderson, 1996; Ghetie and Ward, 2000, 2002) or transcytosis (Roberts *et al.,* 1990; Dickinson *et al.,* 1999; McCarthy *et al.,* 2000; Kobayashi *et al.,* 2002).

Although the pH-dependence of Fc-FcRn binding is clearly documented, the experimental evidence regarding FcRn-mediated internalization by cells at neutral pH is less clear. Although some previous studies report no detectable binding of Fc by cells incubated at pH 7.0–7.4 (Rodewald, 1976, 1980), a number of other studies report that internalization of IgG/Fc by FcRn-expressing cells is enhanced over that of untransfected cells at pH 7.3–7.8 (Claypool *et al.,* 2004; Yoshida *et al.,* 2004; Stirling *et al.,* 2005; Tesar *et al.,* 2006). In one study, similar internalization of IgG from the basolateral surface of MDCK cells was observed at pH 6.0 and 7.3 (Claypool *et al.,* 2004). Evidence of FcRn-mediated internalization of IgG at physiological pH was also presented by Antohe *et al.* (2001), who demonstrated that internalization of radiolabeled IgG by human placental endothelia at pH 7.4 was significantly decreased in the presence of a 100-fold excess of unlabeled IgG.

To investigate the role of FcRn in the early steps of endocytosis of IgG, we developed an experimental model system that allows us to directly visualize and quantify internalization of fluorescent Fc fragments in FcRn-transfected cells during incubation periods brief enough to primarily reflect internalization of Fc. Cultured HULEC-5A lung microvascular endothelia and MDCK cells were transiently transfected with GFP fusion proteins of human FcRn or mouse FcRn. These cells were analyzed by quantitative confocal microscopy after brief incubations with fluorescent conjugates of human Fc molecules. The fluorescently labeled recombinant Fcs bound to FcRn with pH-dependent affinities similar to values published for the corresponding intact IgGs (Firan *et al.,* 2001; Hinton *et al.,* 2004; Datta-Mannan *et al.,* 2007) and similar to unconjugated Fcs (Table 1).

In transiently transfected cells, GFP-FcRn localized to endosomes of the recycling pathway, extensively colocalizing with internalized fluorescent Tf, and excluded from lysosomes. Fluorescent Fc constructs were internalized into these same compartments, from which they recycled. Based on a model of fluid-phase internalization of Fc, one would expect to find similar internalization of fluorescent Fc molecules by transfected and unstransfected cells during the short incubations used in these studies. However, in both HULEC-5A and MDCK cells we consistently found that transfected cells displayed strong internalization of fluorescent Fc into endosomes of the recycling pathway, whereas untransfected neighbors showed almost undetectable internalization. Similar results were found in cells expressing GFP chimeras of either human or mouse FcRn. These results suggested that internalization of Fc might be mediated by interactions with FcRn at the plasma membrane. The possibility that interactions with FcRn significantly contributed to internalization of Fc was suggested not only by the association of internalization with cells expressing GFP-FcRn, but also by the fact that the rank-order of internalization followed the rank-order of FcRn affinity, as predicted by SPR affinity studies.

To evaluate the role of fluid-phase internalization in Fc internalization, cells expressing GFP-FcRn were incubated with both fluorescent Fc and fluorescent dextran. To the degree that Fc is internalized via fluid-phase endocytosis, one would expect internalization in proportion to the fluorescent dextran. However, we found that although internalization of fluorescent dextran is essentially constant over a wide range of FcRn expression levels, internalization of Fc increases sharply with FcRn expression. The disproportionate increase in Fc internalization relative to fluid-phase probes with FcRn expression level suggests that FcRn mediates internalization of FcRn, increasing its concentration beyond that resulting from fluid-phase endocytosis. Indeed, quantitative comparison of the ratio of Fc/dextran fluorescence in individual cells demonstrated that the Fc was concentrated in endosomes relative to dextran in proportion to the level of GFP-FcRn expression. This observation is inconsistent with a model of fluid-phase internalization of Fc, which would predict that the ratio of Fc to dextran should be constant and independent of FcRn expression.

Internalization of the nonbinding H435A mutant was, similar to dextran, found to be independent of FcRn expression level, indicating that the increase in Fc internalization with FcRn depends on binding to FcRn. The significance of FcRn binding to Fc internalization was further demonstrated in studies showing that incubation of cells with excess unlabeled Fc reduced internalization of fluorescent Fc to background levels and abolished the linear relationship between internalization and GFP-FcRn expression. The specificity of this interaction is further indicated by the fact that incubation of cells with an excess of the nonbinding H435A form of Fc had no effect on internalization of fluorescent Fc.

To the degree that Fc internalized by FcRn-expressing cells is protected from proteolysis by binding to FcRn in endosomes, the decreased accumulation of Fc by nontransfected cells might reflect increased rates of Fc proteolysis in nontransfected cells. Similar arguments could be made to explain the reduced accumulation of H435A and of WT Fc in the presence of competitor. However, Fc proteolysis is unlikely to diminish cell-associated Fc fluorescence over the time frame of our incubations. Ward *et al.* (2003) find that the fluorescence of the nonbinding H435A mutant increases in HULEC-5A cells over the course of a 20-min incubation and that its fluorescence is subsequently stable in lysosomal compartments for an additional 40 min. Studies of untransfected cells labeled for 20 min with fluorescent WT Fc or the nonbinding H435A mutant Fc and then imaged over time in the absence of extracellular Fc showed no decrease in Fc fluorescence levels over a 20-min period (data not shown).

Potential Mechanisms of FcRn-mediated Internalization of Fc by Cells Incubated at Near-Neutral pH

Our studies demonstrate that expression of FcRn significantly augments internalization of Fc molecules by HULEC-5A and MDCK cells incubated at neutral pH. These results contradict the common assumption that the preponderance of IgG/Fc internalization at neutral pH results from fluid-phase endocytosis. They also raise the question of how FcRn facilitates internalization of Fc by cells at a pH where in vitro binding is undetectable. The disconnect between the cellular studies and the SPR studies suggests that the cellular context somehow provides an acidic microenvironment in which Fc and FcRn interact during internalization. Cell-mediated acidification of the FcRn microenvironment may explain why, although our system is sensitive enough to detect differences in internalization correlating with 3–10-fold differences in affinity at pH 6.0, no substantial increase in internalization was observed in cells incubated at pH 6.0, a condition in which in vitro affinity is increased over 1000-fold.

Although there are mechanisms by which the local environment of the cell surface can be acidified (e.g., Kovbasnjuk and Spring, 2000; Maouyo *et al.,* 2000), we found no evidence of binding of Fc to FcRn at the surface of cells incubated at 4°C.

Alternatively, early endosomes might provide the acidified microenvironment needed to bind Fc to FcRn. Although FcRn-mediated internalization of Fc was still observed in the presence of bafilomycin and methylamine, it is important to recognize that neither of these agents completely blocks of acidification of early endosomes (Johnson *et al.,* 1993; Presley *et al.,* 1993), thus admitting the possibility that residual acidification is sufficient to support binding of Fc to FcRn in endosomes.

Insofar as binding in endosomes occurs downstream of internalization, it would not result in concentration of Fc relative to fluid phase probes nor enhanced Fc internalization in cells expressing FcRn. However, studies of the early endocytic pathway indicate that the process of internalization is more complex and dynamic than it first appears. Several different laboratories have identified a fast recycling pathway whose magnitude indicates that internalization is not a simple, vectorial process, but rather one in which membrane and volume are rapidly and repeatedly internalized and recycled from early endosomes (Besterman, 1981; Sheff *et al.,* 1999; Hao and Maxfield, 2000). Thus Fc internalized in fluid-phase may be repeatedly internalized into acidic endosomes, where it might bind to FcRn. To the degree that FcRn binding results in retention of Fc in endosomes, Fc will accumulate in an early endosome with each iteration of the internalization step, up the point where all of the FcRn in the endosome are occupied by Fc. There are two ways that binding to FcRn might result in endosomal retention of Fc. First, membranes containing FcRn may not participate in the fast recycling pathway to the same degree as other membranes in early endosomes. So, for example, there may be reservoirs of FcRn on endosomal subdomains, or binding of Fc to FcRn might physically sequester the resulting complex from the fast recycling pathway. Alternatively, Fc:FcRn complexes may recycle back to the plasma membrane, but because of the relatively slow rate of dissociation (Ober *et al.,* 2004a), may fail to dissociate before reinternalization. This second model is consistent with the studies of Ober *et al.* (2004a), which suggest a kiss-and-run model (Lencer and Blumberg, 2005) in which a fraction of Fc–FcRn complexes are reinternalized after recycling.

CONCLUSIONS

The studies presented here demonstrate that FcRn mediates concentrative internalization of Fc from a neutral pH environment, even at Fc concentrations well below the estimated K_d of binding to FcRn at neutral pH. These results suggest that FcRn receptor–mediated internalization of IgG may be physiologically important not only for cells internalizing IgG from an acidic space, such as intestinal epithelia, but also for endothelial cells participating in homeostatic regulation of circulating IgG levels where IgG would be internalized from a neutral environment. Compared with a simple mechanism of fluid-phase uptake, a process of concentrative internalization would provide a more efficient method of IgG uptake that would minimize the amount of bulk fluid that must be processed by a cell in order to accomplish surveillance and regulation of circulating IgG levels. Although we have demonstrated that FcRn-mediated internalization of IgG can be significant in cells expressing abundant FcRn, the physiological significance of FcRn-mediated internalization of IgG may vary between cell types, species, and IgG-FcRn combinations. For example, FcRn-mediated internalization of IgG may be less significant in cells expressing less FcRn or in cells that are especially active in pinocytosis.

The mechanism by which FcRn mediates internalization of IgG is not clear, although we have suggested possible mechanisms involving iterative internalization and binding of Fc to FcRn in endosomes. The rationale for the apparently specialized mechanism of IgG internalization may be that it provides a solution to the problem of accomplishing efficient IgG uptake while at the same time providing for efficient release of IgG after recycling. In this sense, FcRn is similar to the transferrin receptor, which accomplishes the trick of both efficiently binding Tf for internalization and releasing Tf after recycling via orchestrated changes in transferrin affinity as it trafficks through the cell. A process of iterative binding in endosomes may provide a method by which FcRn can facilitate both concentrative internalization and recycling of IgG. Future studies will be required to test the model of iterative internalization, a process that may have general utility for receptor-ligand systems with pH-dependent binding.

REFERENCES

Antohe, F., Radulescu, L., Gafencu, A., Ghetie, V., and Simionescu, M. (2001). Expression of functionally active FcRn and the differentiated bidirectional transport of IgG in human placental endothelial cells. Hum. Immunol. *62,* 93–105.

Besterman, J. M., Airhart, J. A., Woodworth, R. C., and Low, R. B. (1981). Exocytosis of pinocytosed fluid in culture cells: kinetic evidence for rapid turnover and compartmentation. J. Cell Biol. *91,* 716–727.

Borvak, J., Richardson, J., Medesan, C., Antohe, F., Radu, C., Simionescu, M., Ghetie, V., and Ward, E. S. (1998). Functional expression of the MHC class I-related receptor, FcRn, in endothelial cells of mice. Int. Immunol. *10,* 1289–1298.

Brown, P. S., Wang, E., Aroeti, B., Chapin, S. J., Mostov, K. E., and Dunn, K. W. (2000). Definition of distinct compartments in polarized Madin-Darby canine kidney (MDCK) cells for membrane-volume sorting, polarized sorting and apical recycling. Traffic *1,* 124–140.

Claypool, S. M., Dickinson, B. L., Wagner, J. S., Johansen, F. E., Venu, N., Borawski, J. A., Lencer, W. I., and Blumberg, R. S. (2004). Bidirectional

transepithelial IgG transport by a strongly polarized basolateral membrane Fc gamma-receptor. Mol. Biol. Cell *15*, 1746–1759.

Dall' Acqua, W. F., Woods, R. M., Ward, E. S., Palaszynski, S. R., Patel, N. K., Brewah, Y. A., Wu, H., Kiener, P. A., and Langermann, S. (2002). Increasing the affinity of a human IgG1 for the neonatal Fc receptor: biological consequences. J. Immunol. *169*, 5171–5180.

Datta-Mannan, A., Witcher, D. R., Tang, Y., and Wroblewski, V. J. (2007a). Humanized IgG1 variants with differential binding properties to the neonatal Fc receptor: relationship to pharmacokinetics in mice and primates. Drug Metab. Dispos. *35*, 86–94.

Datta-Mannan, A., Witcher, D. R., Tang, Y., Watkins, J., and Wroblewski, V. J. (2007b). Monoclonal antibody clearance. Impact of modulating the interaction of IgG with the neonatal Fc receptor. J. Biol. Chem. *282*, 1709–1717.

Dickinson, B., Badizadegan, K., Wu., Z., Ahouse, J., Zhu, X., Simister, N., Blumberg, R., and Lencer, W. (1999). Bidirectional FcRn-dependent IgG transport in a polarized human intestinal epithelial cell line. J. Clin. Inv. *104*, 903–911.

Dunn, K., Park, J., Semrad, C., Gelman, D., Shevell, T., and T. McGraw. (1994). Regulation of endocytic trafficking and acidification are independent of the cystic fibrosis transmembrane regulator. J. Biol. Chem. *269*, 5336–5345.

Firan, M., Bawdon, R., Radu, C., Ober, R. J., Eaken, D., Antohe, F., Ghetie, V., and Ward, E. S. (2001). The MHC class I-related receptor, FcRn, plays an essential role in the maternofetal transfer of γ-globulin in humans. Int. Immunol. *13*, 993–1002.

Ghetie, V., Hubbard, J. G., Kim, J.-K., Tsen, M.-F., and Ward, E. S. (1996). Abnormally short serum half-lives of IgG in β2-microglobulin-deficient mice. Eur. J. Immunol. *26*, 690–696.

Ghetie, V., and Ward, E. S. (2000). Multiple roles for the major histocompatibility complex class I- related receptor FcRn. Annu. Rev. Immunol. *18*, 739–766.

Ghetie, V., and Ward, E. S. (2002). Transcytosis and catabolism of antibody. Immunol. Res. *25*, 97–113.

Gurbaxani, B., Dela Cruz, L. L., Chintalacharuvu, K., and Morrison, S. L. (2006). Analysis of a family of antibodies with different half-lives in mice fails to find a correlation between affinity for FcRn and serum half-life. Mol. Immunol. *43*, 1462–1473.

Hao, M., and Maxfield, F. (2000). Characterization of rapid membrane internalization and recycling. J. Biol. Chem. *275*, 15279–15286.

Haymann, J.-P., Levraud, J.-P., Bouet, S., Kappes, V., Hagege, J., Nguyen, G., Xu, Y., Rondeau, E., and Sraer, J.-D. (2000). Characterization and localization of the neonatal Fc receptor in adult human kidney. J. Am. Soc. Nephrol. *11*, 632–639.

Hinton, P. R., *et al.* (2004). Engineered human IgG antibodies with longer serum half-lives in primates. J. Biol. Chem. *279*, 6213–6216.

Israel, E. J., Taylor, S., Wu, Z., Mizoguchi, R. S., Blumberg, R. S., Bhan, A., and Simister, N. E. (1997). Expression of the neonatal Fc receptor, FcRn, on human intestinal epithelial cells. Immunology *92*, 69–74.

Israel, E. J., Wilsker, D. F., Hayes, K. C., Schoenfeld, D., and Simister, N. E. (1996). Increased clearance of IgG in mice that lack beta 2-microglobulin: possible protective role of FcRn. Immunology *89*, 573–578.

Johnson, L. S., Dunn, K. W., and McGraw, T. E. (1993). Endosome acidification and receptor trafficking: bafilomycin A1 slows receptor externalization by a mechanism involving the receptor's internalization motif. Mol. Biol. Cell *4*, 1251–1266.

Junghans, R. P., and Anderson, C. L. (1996). The protection receptor for IgG catabolism is the β2-microglobulin-containing neonatal intestinal transport receptor. Proc. Natl. Acad. Sci. USA *93*, 5512–5516.

Kobayashi, N., Suzuki, Y., Tsuge, T., Okumura, K., Ra, C., and Tomino, Y. (2002). FcRn-mediated transcytosis of immunoglobulin G in human renal proximal tubular epithelial cells. Am. J. Physiol. Renal Physiol. *282*, F358–F365.

Kovbasnjuk, O. N., and Spring, K. R. (2000). The apical membrane glycocalyx of MDCK cells. J. Membr. Biol. *176*, 19–29.

Lencer, W. I., and Blumberg, R. S. (2005). A passionate kiss, then run: exocytosis and recycling of IgG by FcRn. Trends Cell Biol. *15*, 5–9.

Maouyo, D., Chu, S., and Montrose, M. H. (2000). pH heterogeneity at intracellular and extracellular plasma membrane sites in HT29–C1 monolayers. Am. J. Physiol. Cell Physiol. *278*, C973–C981.

Maxfield, F. R., and Dunn, K. W. (1990). Studies of endocytosis using image intensification fluorescence microscopy and digital image analysis. In: Optical Microscopy for Biology, ed. B. Herman and K. Jacobsen, New York: Alan R. Liss, 357–371.

McCarthy, K. M., Yoong, Y., and Simister, N. E. (2000). Bidirectional transcytosis of IgG by the rat neonatal Fc receptor expressed in a rat kidney cell line: a system to study protein transport across epithelia. J. Cell Sci. *113*, 1277–1285.

Ober, R. J., Radu, C. G., Ghetie, V., and Ward, E. S. (2001). Differences in promiscuity for antibody-FcRn interactions across species: implications for therapeutic antibodies. Int. Immunol. *13*, 1551–1559.

Ober, R. J., Martinez, C., Lai, X., Zhou, J., and Ward, E. S. (2004a). Exocytosis of IgG as mediated by the receptor, FcRn: an analysis at the single-molecule level. Proc. Natl. Acad. Sci. USA *101*, 11076–11081.

Ober, R. J., Martinez, C., Vaccaro, C., Zhou, J., and Ward, E. S. (2004b). Visualizing the site and dynamics of IgG salvage by the MHC class I-related receptor, FcRn. J. Immunol. *172*, 2021–2029.

Praetor, A., Ellinger, I., and Hunziker, W. (1999). Intracellular traffic of the MHC class-1-like IgG Fc receptor, FcRn, expressed in epithelial MDCK cells. J. Cell Sci. *112*, 2291–2299.

Presley, J., Mayor, S., Dunn, K., Johnson, L., McGraw, T., and Maxfield, F. (1993). The End2 mutation in CHO cells slows the exit of transferrin receptors from the recycling compartment but bulk trafficking is unaffected. J. Cell Biol. *122*, 1231–1241.

Raghavan, M., Bonagura, V. R., Morrison, S. L., and Bjorkman, P. J. (1995). Analysis of the pH dependence of the neonatal Fc receptor/immunoglobulin G interaction using antibody and receptor variants. Biochemistry *34*, 14649–14657.

Roberts, D. M., Guenthert, M., and Rodewald, R. (1990). Isolation and characterization of the Fc receptor from the fetal yolk sac of the rat. J. Cell Biol. *111*, 1867–1876.

Rodewald, R. (1976). pH-dependent binding of immunoglobulin to intestinal cells of the neonatal rat. J. Cell Biol. *71*, 666–669.

Rodewald, R. (1980). Distribution of immunoglobulin G receptors in the small intestine of the young rat. J. Cell Biol. *85*, 18–32.

Rodewald, R., and Kraehenbuhl, J.-P. (1984). Receptor-mediated transport of IgG. J. Cell Biol. *99*, 159s–164s

Sakagami, M., Omidi, Y., Campbell, L., Kandalaft, L. E., Morris, C. J., Barar, J., and Gumbleton, M. (2006). Expression and transport functionality of FcRn within rat alveolar epithelium: a study in primary cell culture and in the isolated perfused lung. Pharmaceut. Res. *23*, 270–279.

Sheff, D., Daro, E., Hull, M., and Mellman, I. (1999). The receptor recycling pathway contains two distinct populations of early endosomes with different sorting functions. J. Cell Biol. *145*, 123–139.

Sokal, R. and Rohlf, J. (1995) Biometry: The Principles and Practice of Statistics in Biological Research, San Francisco: W. H. Freeman.

Spiekermann, G. M., Finn, P. W., Ward, E. S., Dumont, J., Dickinson, B. L., Blumberg, R. S., and Lencer, W. I. (2002). Receptor-mediated immunoglobulin G transport across mucosal barriers in adult life: functional expression of FcRn in the mammalian lung. J. Exp. Med. *196*, 303–310.

Stirling, C.M.A., Charleson, B., Takamatsu, H., Claypool, S., Lencer, W., Blumberg, R. S., and Wileman, T. E. (2005). Characterization of the porcine neonatal Fc receptor—potential use for trans-epithelial protein delivery. Immunology *114*, 542–553.

Story, C. M., Mikulska J. E., and Simister, N. E. (1994). A major histocompatibility complex class I-like Fc receptor cloned from human placenta: possible role in transfer of immunoglobulin G from mother to fetus. J. Exp. Med. *180*, 2377–2381.

Telleman, P., and Junghans, R. P. (2000). The role of the Brambell receptor (FcRB) in liver: protection of endocytosed immunoglobulin G (IgG) from catabolism in hepatocytes rather than transport of IgG to bile. Immunol *100*, 245–251.

Tesar, D. B., Tiangco, N. E., and Bjorkman, P. J. (2006). Ligand valency affects transcytosis, recycling and intracellular trafficking mediated by the neonatal Fc receptor. Traffic *7*, 1–16.

van Weert, A., Dunn, K., Geuze, H., Maxfield, F., and Stoorvogel, W. (1995). Transport from late endosomes to lysosomes, but not sorting of integral membrane proteins in endosomes, depends upon the vacuolar proton pump. J. Cell Biol. *130*, 821–834.

Vidarsson, G., Stemerding, A. M., Stapleton, N. M., Spliethoff, H. J., Rebers, F.E.M., deHaas, M., and van de Winkel, J.G.J. (2006). FcRn: an IgG receptor on phagocytes with a novel role in phagocytosis. Blood *108*, 3573–3579.

Waldmann, T. A., and Strober, W. (1969). Metabolism of immunoglobulins. Prog. Allergy *13*, 1–110.

Wallace, K. H., and Rees, A. R. (1980). Studies on the immunoglobulin-G Fc-fragment receptor from neonatal rat small intestine. Biochem. J. *188*, 9–16.

Wang, E., Brown, P. S., Aroeti, B., Chapin, S. J., Mostov, K. E., and Dunn, K. W. (2000). Apical and basolateral endocytic pathways of MDCK cells meet in acidic common endosomes distinct from a nearly-neutral apical recycling endosome. Traffic 1, 480–493.

Wani, M. A., Haynes, L. D., Kim, J., Bronson, C. L., Chaudhury, C., Mohanty, S., Waldmann, T. A., Robind, J. M., and Anderson, C. L. (2006). Familial hypercatabolic hypoproteinuria caused by deficiency of the neonatal Fc receptor, FcRn, due to mutant beta-2-microglobulin gene. Proc. Natl. Acad. Sci. USA 103, 5084–5089.

Ward, E. S., Martinez, C., Vaccaro, C., Zhou, J., Tang, Q., and Ober, R. J. (2005). From sorting endosomes to exocytosis: association of Rab4 and Rab11 GTPases with the Fc receptor, FcRn, during recycling. Mol. Biol. Cell 16, 2028–2038.

Ward, E. S., Zhou, J., Ghetie, V., and Ober, R. J. (2003). Evidence to support the cellular mechanism involved in serum IgG homeostasis in humans. Int. Immunol. 15, 187–195.

Yamashiro, D., Tycko, B., Fluss, S., and Maxfield, F. (1984). Segregation of transferrin to a mildly acidic (pH 6.5) para-Golgi compartment in the recycling pathway. Cell 37, 789–800.

Yoshida, M., Claypool, S., Wagner, J., Mizoguchi., E., Roopenian, D., Lencer, W., and Blumberg, R. (2004). Human neonatal Fc receptor mediates transport of IgG to luminal secretions for delivery of antigens to mucosal dendritic cells. Immunity 20, 769–783.

Zhou, J., Johnson, J. E., Ghetie, V., Ober, R. J., and Ward, E. S. (2003). Generation of mutated variants of the human form of the MHC Class I-related receptor, FcRn, with increased affinity for mouse immunoglobulin G. J. Mol. Biol. 332, 901–913.

Zhu, X. et al. (2001). MHC class I-related neonatal Fc receptor for IgG is functionally expressed in monocytes, intestinal macrophages, and dendritic cells. J. Immunol. 166, 3266–3276.